A Tracking Fiber Detector based on Silicon Photomultipliers for the KAOS Spectrometer

S. Sánchez Majos, P. Achenbach, and J. Pochodzalla

***Abstract*—A tracking detector based on two meters long scintillating fibers read out by silicon photomultipliers (SiPM) is being developed for the KAOS spectrometer at the Mainz Microtron MAMI. Results from a prototype setup using 2 mm square fibers and large area SiPM readout are presented. The detection efficiency of such a combination was measured to be between 83 and 100% depending on the threshold on the SiPM amplitude. A Monte Carlo simulation based on a physical model was employed in order to extract the photon detection efficiency of the SiPM devices.**

***Index Terms*—Silicon Photomultipliers, Particle Detection Efficiency, Tracking Detectors.**

I. INTRODUCTION

THE recently upgraded electron accelerator MAMI-C with beam energies up to 1.5 GeV has opened the door to kaon production experiments at the Institut für Kernphysik in Mainz, Germany [1]. The short orbit spectrometer KAOS has been added to the existing facilities allowing the detection of short living kaons with a high survival probability. The simultaneous detection of scattered electrons and positive kaons with this instrument at very forward angles will permit spectroscopic studies of hypernuclei by missing mass reconstruction. The spectrometer was successfully operated at GSI near Darmstadt in heavy ion collision experiments. In order to cope with the planned experiments at MAMI the existing detector system has to be completed with a package for the electron momentum and track reconstruction. Timing and position information can be obtained simultaneously by scintillating fiber tracking detectors. Multianode photomultipliers (MaPMT) have been used as readout devices for the vertical component of a detector of this type. Experience has shown that there are several drawbacks associated with MaPMT. In particular, optical cross-talk among neighboring channels has been observed giving rise to a reduced position resolution [2]. In addition the need for high voltage supplies and magnetic shielding increases the overall price and complexity of the detector [3].

Moreover, a light sensor for the horizontal component of the tracking detector has to be capable of a reliable operation in vacuum. Silicon photomultipliers (SiPM) are emerging as a solid state alternative to conventional photomultipliers in many fields. Hundreds of micrometric avalanche photodiodes (APD) connected in parallel are operated in a SiPM beyond the breakdown voltage for a high gain of 10^6 [4].

Manuscript received November 14, 2008. Work supported in part by GSI as F+E project MZPOCH.

The authors are with the Institut für Kernphysik, Johannes Gutenberg-Universität, Mainz, Germany (e-mail: sanchez@kph.uni-mainz.de, patrick@kph.uni-mainz.de, pochodza@kph.uni-mainz.de)

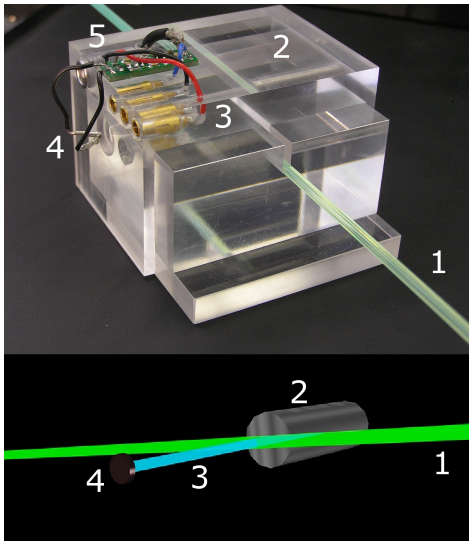

Fig. 1. Modular Plexiglas device used for measurements of the SiPM/fiber performance. The two meters long green emitting fiber (1) is placed in a slit and kept in place by the top Plexiglas cover. A lead collimator (2) containing an ^{90}Sr beta source with an opening of 0.7 mm is inserted in the central block perpendicular to the square fiber in good alignment with its center. The fraction of electrons that cross the first fiber penetrate a short blue emitting fiber (3) collinear with the collimator axis. The signal from this trigger fiber is read out by a blue sensitivity SiPM (4) and amplified by a transimpedance integrated amplifier (5).

II. SCINTILLATING FIBERS WITH SIPM READOUT AS TRACKING DETECTORS

SiPM have been suggested as possible readout device for the 150 two meters long scintillating fibers forming the horizontal detector. Magnetic field insensitivity, small volume, sensor independence, good vacuum performance and low voltage operation make SiPM interesting for this application. Low light level detection is on the other hand challenging for these devices due to their high dark count rate. Long and thin fibers will only be capable of guiding a few photons to the detector surface due to the low energy deposition of minimum ionizing electrons and the strong light absorption. Detection efficiency is a major issue for a tracking system and the right combination of fiber and SiPM has to be carefully studied. Radiation hardness studies have also been performed showing that commercially available SiPM suffer from a large increase in leakage current for relatively low radiation doses [5]. This poses an additional problem for their use in combination with long scintillator fibers. The leakage current will appear as a high rate of single photoelectron signals due to the avalanche amplification specific of photodiodes operated in the limited

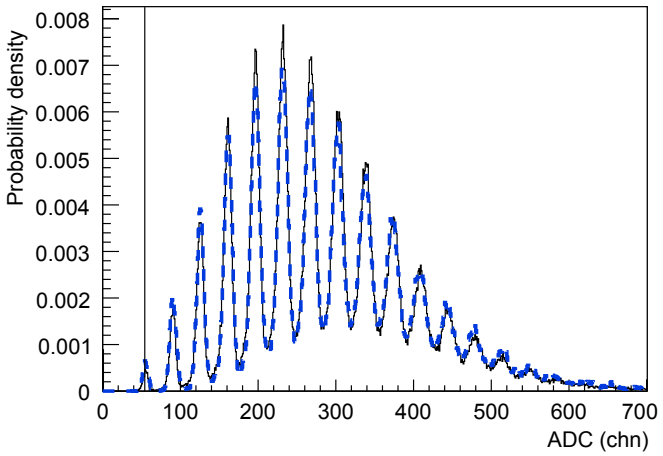

Fig. 2. ADC spectrum for a Photonique device of 1 mm^2 cross-section with type number SSPM-0701BG-TO18 illuminated by a low intensity light source. The position of the pedestal peak is indicated by a vertical line, the following peaks resolve the signals from single and multiple pixels of the SiPM. The peak structure is due to the narrow response function. The bold-dashed curve is the result of a Monte Carlo simulation including the main operating parameters of SiPM.

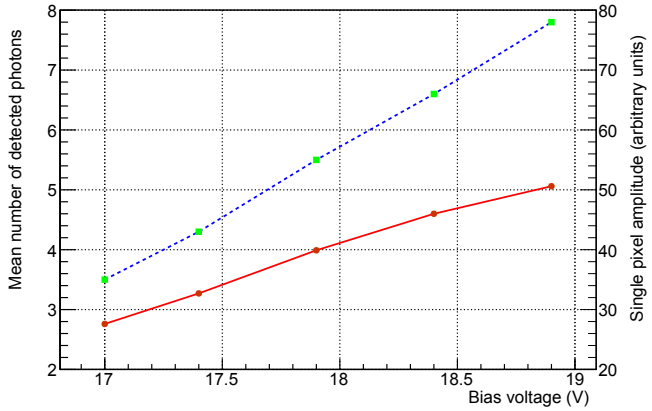

Fig. 3. Mean number of detected photons and single pixel amplitude as a function of the bias voltage for two Photonique devices of 1 mm^2 cross-section with type number SSPM-0701BG-TO18. The observed differences between the two curves are not fully understood but manufacturing variability seems to be the most probable explanation. The measured linear dependence is explained by the linear increase in avalanche probability and diode capacity charging.

Geiger mode.

Fig. 2 shows a typical ADC spectrum recorded for a 1 mm^2 device from Photonique[1], type number SSPM-0701BG-TO18. The bold-dashed curve is the result of a Monte Carlo simulation including the most relevant parameters of SiPM as optical cross-talk, after-pulsing, photon detection efficiency (PDE) and gain variations developed in order to extract the mean number of detected photons. This method is necessary due to the overestimation that is quoted in many publications where the effect of optical cross-talk and after-pulsing is not subtracted. SiPM are manufactured so that signal uniformity from pixel to pixel is quite good, typically within 10%. The small gain variation together with the narrow single electron response function of each APD provides excellent photon counting capabilities as can be appreciated in the well defined peak structure of the spectrum.

It is well known that SiPM noise rate is mostly due to single pixel signal. Rates of the order of several megahertz at room temperature are normal in todays commercially available SiPM. An avalanche of 10^6 carriers in any of the micrometric APD forming the SiPM will create around 50 photons via hot carrier luminescence with enough energy to trigger any neighboring pixel [6]. This phenomenon is known as optical cross-talk and explains the measurable dark rate for threshold beyond one pixel signal amplitude. These signals compete with real signals generated by a small number of photons. A simple model based on the probability q of single neighbor activation allows the probabilities for the different clusters of APD to be calculated (only pixels sharing one complete side are allowed as members of a cluster). Cluster probabilities are given by the zero pixel cross-talk probability $P(0) = (1-q)^4$, and the N-pixel cross-talk probabilities $P(1) = 4q(1-q)^6$, $P(2) = q^2[6(1-q)^8 + 12(1-q)^7]$, and $P(3) = q^3[32(1-q)^8 + 32(1-q)^9 + 8(1-q)^{10}]$.

[1]Photonique SA, http://www.photonique.ch (2008)

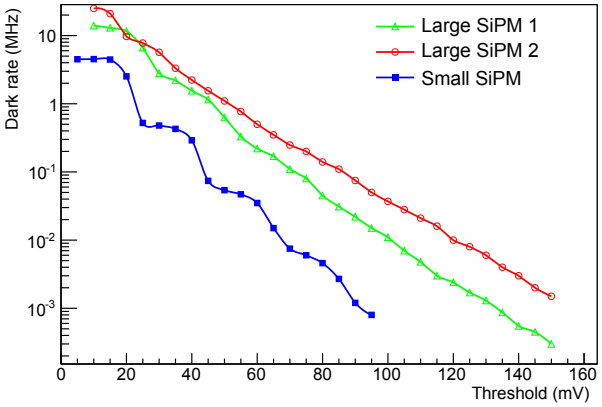

Fig. 4. Dark count rate as a function of threshold level measured for two large area SiPM SSPM-0606BG4MM-PCB and for a 1 mm^2 device. The dark count rate is a factor of four higher for the larger devices and steps are less defined due to the more probable signal pile-up.

III. Measurements on SiPM Performance

Previous studies performed with 0.85 mm diameter 2 m long cylindrical fibers read out by Photonique SiPM with an active area of 1 mm^2 showed that the small number of generated photons was a serious concern for efficient electron detection. Fig. 3 shows the mean ADC value as function of the applied voltage for this SiPM. The almost liner dependency allows to conclude that low voltages are more appropriate for low light level detection due the much faster increase (exponential) in the dark count rate with voltage. The differences in the measurements for the two devices are not fully understood although manufacturing variability seems to be the most probable explanation. A larger energy deposition in the scintillating material is necessary in order to achieve detection efficiencies close to 100%. On the other hand a

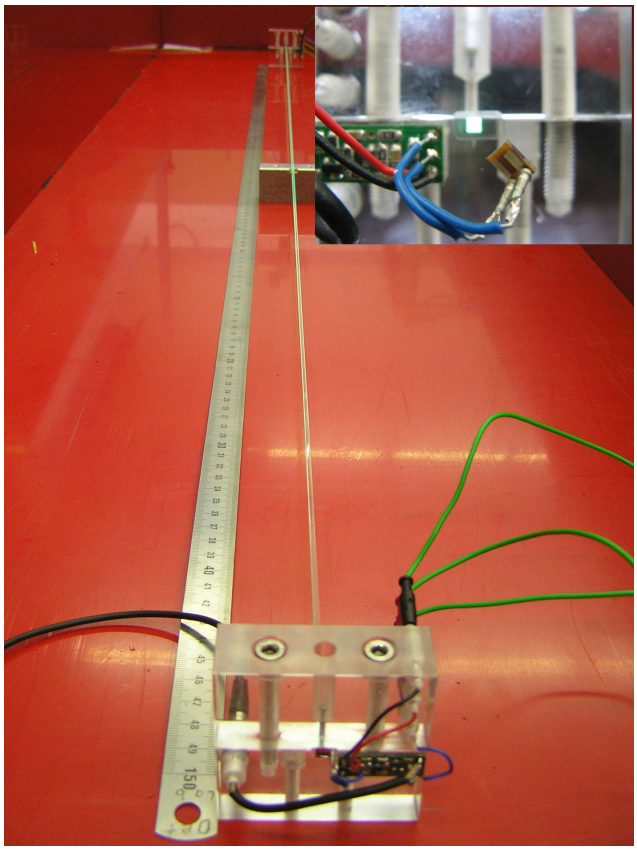

Fig. 5. Test setup inside a light tight box containing the two meter long fiber under study. The inset shows the transparent connectors on both extremes that allow optimal alignment of SiPM and fiber. No specific optical coupling was necessary due to the good matching of indexes of refraction of the protective epoxy layer of the SiPM and the fiber core material.

minimum particle trajectory disturbance is important for a tracking detector.

2 mm square fibers (emission peak at 492 nm) with double cladding from Bicron[2] with type number BCF-20 were considered an adequate compromise for the application. For the chosen fiber the manufacturer quoted a value of 7.3% trapping efficiency. For the SSPM-0606BG4MM-PCB device typical PDE values range from 15 to 25% with the PDE almost constant over the wavelength range 500–650 nm. However, the PDE is linear function of the bias voltage due to the increase in probability of avalanche initiation. The typical bias voltage for these devices is 30 V. The maximum number of detected photons from such a combination can be estimated with the above values to be of the order of 12 photons.

The measured dark count rate as a function of the threshold level in a leading edge discriminator is shown for the two 4.4 mm^2 and for a 1 mm^2 device in Fig. 4. The step like structure can be explained by the cross-talk probabilities discussed above. For large area devices steps are much less defined due to signal pile-up. It is clear from this measurement

[2]Bicron, http://www.bicron.com (2008)

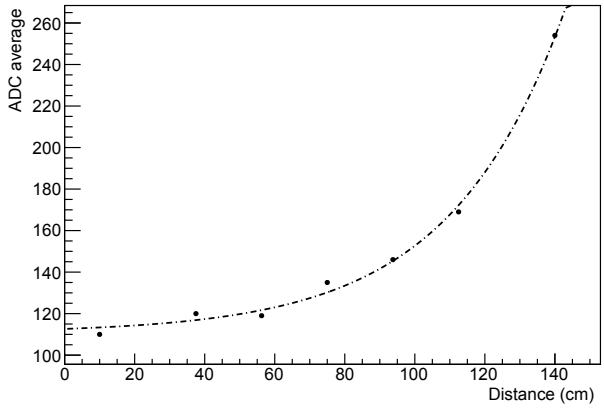

Fig. 6. Mean ADC value measured as a function of the beta source position. A characteristic exponential dependence is observed but the attenuation length seems to substantially smaller than the value quoted by the manufacturer.

that the threshold level is a crucial issue for noise reduction. Fibers of 4 mm^2 cross-section will only increase the amount of generated light by a factor of 2 but noise in the SiPM will be 4 times larger due to the fact that dark count rate increases linearly with the detector surface. The improvement comes from the fact that high efficiencies can be achieved with higher thresholds for the larger cross-section fibers and the geometrical reduction of dark count rate with threshold level will allow an effectively lower rate.

Fig. 5 shows the setup for characterizing a two meters long Bicron BCF-20 fiber read out in both extremes by the large area SiPM. Signals are brought into a compact electronic board incorporating a SiPM bias circuit and a transimpedance amplifier optimized for the amplification of SSPM signals. The coupling to the scintillating fiber is direct. No optical connection is necessary due to the small difference in the refraction indexes of the protecting epoxy layer used for the SiPM and the fiber core material. A Plexiglas connector was designed that allowed a reliable connection and mechanical stability of the full assembly as well as optical control of the relative position of fiber to SiPM for a proper alignment. A 250 cm long light tight box was constructed to keep the experimental arrangement protected from external light sources. The voltage for the preamplifiers and the SiPM was constantly monitored and the temperature was measured to be stable within 2 °C. Light absorption was measured by exciting the fiber at several points with a beta source and by determining the corresponding change in the mean ADC value, see Fig. 6. The measured absorption length of 1.5 m is substantially smaller than the value quoted by the manufacturer ($>$ 3.5 m for 1 mm diameter fiber measured with a bialkali cathode PMT) which needs clarification.

A simple calculation shows the equivalence of the energy loss in scintillating fiber tests made with the ^{90}Sr source to the loss of high energy electrons. ^{90}Sr is an beta-source with a maximum kinetic energy of $E_{max} = 546$ keV and a mean kinetic energy of $E = 196$ keV. It decays to ^{90}Y with a half-life of 29.12 y. The short-lived daughter decays with a maximum kinetic energy of $E_{max} = 2.28$ MeV and a mean

TABLE I

MEASURED PARTICLE DETECTION EFFICIENCIES FOR 2 MM SQUARE FIBERS AND 0.86 MM CYLINDRICAL FIBERS BEING READ OUT BY SIPM AS A FUNCTION OF THRESHOLD VALUE IN UNITS OF SINGLE PIXEL AMPLITUDE. THE RANDOM COINCIDENCE RATE WAS DETERMINED FROM DARK COUNT RATE MEASUREMENTS.

	2 mm Fiber / 4.4 mm^2 SiPM		0.86 mm Fiber / 1 mm^2 SiPM	
Threshold (pixel)	Efficiency (%)	Random Rate (kHz)	Efficiency (%)	Random Rate (kHz)
0.5	100	2 000	91	320
1.5	99.8	80	76	5
2.5	95.0	1.3	56	0.45
3.5	82.6	0.04	35	0.04

energy of $E = 933$ keV. The spectra of both decays are shown in Fig. 7. Most electrons from the ^{90}Sr decay are stopped in a 2 mm thick scintillator, since the range of 0.35 MeV electrons in scintillator material is only $R = 1$ mm. It is readily seen from the stopping power curves that ionizing energy loss of the ~ 1 MeV electrons from ^{90}Y decay will be equivalent to that of high energy electrons.

The efficiency was measured with a dedicated device consisting of a 3 cm long cylindrical lead collimator with an aperture of 0.7 mm in diameter and containing a ^{90}Sr beta source, see Fig. 1. Electrons were forced to cross the 2 m long fiber by a Plexiglas structure with a slit to accommodate the studied fiber. A 2 cm long blue scintillating fiber was introduced in the Plexiglas parallel to the electron trajectory so that those that are able to go through the studied fiber will enter longitudinally the small one depositing all their remaining energy there. The relatively large amount of generated photons is detected by a blue sensitive Photonique device with type number SSPM-0611B1MM-TO18. The signal amplifier is located in the Plexiglas block as well so that a very compact device was obtained that could be freely moved along the fiber. Practically no absorption takes place in the 2 cm short trigger fiber and high thresholds for the trigger discriminator could be chosen. The background rate in absence of the exciting source was almost zero. Efficiency was defined as the quotient of trigger signals to coincidences of the left and right large area SiPM. This value was studied as a function of the threshold level in units of single pixel signals. The results for the cylindrical and square fibers are shown in Table I.

IV. CONCLUSION

The KAOS spectrometer at MAMI will be extended by a large fiber detector in the near future. Our study has shown that the readout of 2 mm square scintillating fibers by SiPM can lead to near 100% detection efficiency for electrons. A random coincidence rate for a setup of two 4.4 mm^2 large area SiPM is unavoidable because of high dark count rate of these devices. However, with a reasonable threshold setting and further trigger conditions such a system is feasable.

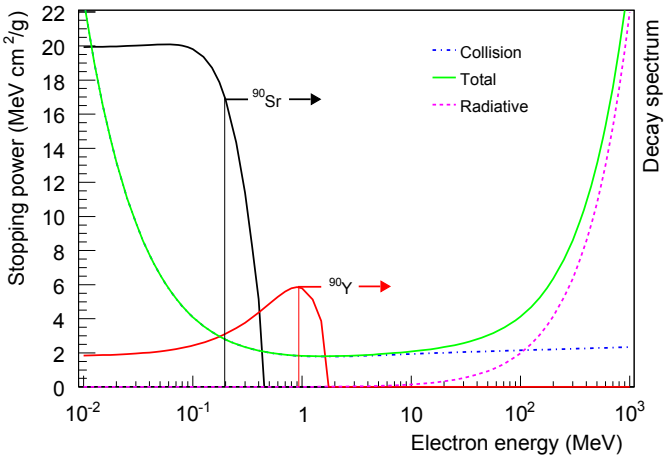

Fig. 7. Stopping power of organic fibers for electrons separated into collision, radiative and total losses as a function of energy. The decay spectra of ^{90}Sr and ^{90}Y and the mean kinetic energy of the decay electrons were overlaid onto this plot.

REFERENCES

[1] K.-H. Kaiser *et al.*, "The 1.5 GeV harmonic double-sided microtron at Mainz University," *Nucl. Instrum. Meth. Phys. Res.*, vol. A 593, pp. 159–170, August 2008.

[2] P. Achenbach *et al.*, "In-beam tests of scintillating fibre detectors at MAMI and at GSI," *Nucl. Instrum. Meth. Phys. Res.*, vol. A 593, pp. 353–360, August 2008.

[3] P. Achenbach *et al.*, "New detectors for the kaon and hypernuclear experiments with KAOS at MAMI and with $\bar{\text{P}}$ANDA at GSI," in *Proceedings of the IX International Symposium on Detectors for Particle, Astroparticle and Synchrotron Radiation Experiments, SLAC, 3–6 April 2006*, V. Luth, Ed. eConf C0604032, 2006, p. 144.

[4] P. Buzhan *et al.*, "An advanced study of silicon photomultiplier," *ICFA Instrum. Bull.*, vol. 23, pp. 28–41, 2001.

[5] S. Sánchez Majos *et al.*, "Noise and radiation damage in silicon photomultipliers exposed to electromagnetic and hadronic radiation," *Nucl. Instrum. Meth. Phys. Res.*, vol. A 602, pp. 506–510, 2009.

[6] N. Otte, "The silicon photomultiplier—a new device for high energy physics, astroparticle physics, industrial and medical applications," in *Proceedings of the IX International Symposium on Detectors for Particle, Astroparticle and Synchrotron Radiation Experiments, SLAC, 3–6 April 2006*, V. Luth, Ed. eConf C0604032, 2006, p. 18.